Bulletin of the JSME Vol.15, No.3, 2020
Journal of Thermal Science and Technology

Flame-spread behavior of biodiesel (B20) in a microgravity environment

Herman SAPUTRO*, Laila FITRIANA**, Fudhail A MUNIR*** and Masato MIKAMI****

*Department of Mechanical Engineering Education, Universitas Sebelas Maret
Jl. Ahmad Yani No.200, Pabelan, Surakarta, 57169 Indonesia
E-mail: hermansaputro@staff.uns.ac.id
**Department of Mathematic Education, Universitas Sebelas Maret
Jl. Ir. Sutami 36A, Surakarta, 57126 Indonesia
***Faculty of Mechanical Engineering, Universiti Teknikal Malaysia Melaka
Hang Tuah Jaya, Durian Tunggal Melaka, 76100, Malaysia
****Graduate School of Sciences and Technology for Innovation, Yamaguchi University
Tokiwadai, Ube, Yamaguchi, 755-8611 Japan

Received: 16 May 2020; Revised: 6 July 2020; Accepted: 27 July 2020

Abstract

Indonesia has implemented a policy of using diesel fuel containing 20 percent biofuel (commonly known as B20 biodiesel), as stated in Energy and Mineral Resources Ministerial Decree No. 23/2013. This study investigated the flame-spread characteristics of biodiesel (B20) in a microgravity environment through drop tower facilities. This is due to the difficulty in creating droplet sizes similar to the real liquid sprays in the combustion chamber of diesel engines. The experiment used biodiesel (B20) droplets with a diameter 1 mm. The results show that the biodiesel (B20) droplets have characteristics of a flame–spread limit distance $S_{BC}/d_{C0limit} = 7$. This paper discusses the characteristics of biodiesel (B20) droplets in detail.

Keywords : Flame spread behavior, Biodiesel (B20), Microgravity environment

1. Introduction

In September 2018, Indonesia adopted a policy of using diesel fuel containing 20 percent biofuel (commonly known as biodiesel (B20)) specifically for diesel engines, as stated in Energy and Mineral Resources Ministerial Decree No. 23/2013, as part of government efforts to reduce the impact of the currency crisis and high oil prices. Using Biodiesel B20 in diesel engines has several benefits such as cost savings, low emissions, improved engine performance, and fuel compatibility (National Renewable Energy Laboratory, 2009). Biodiesel B20 also meets the Environment Protection Act (EP Act) standard.

Various studies on biodiesel have been carried out such as Biodiesel production (Suresh et al., 2018; Ambat et al., 2018; and Knothe et al., 2017), Stability of biodiesel (Saluja et al., 2016) and Biodiesel on engine performance and emissions (Nabil et al., 2018 and Kumar et al., 2018). Associated with biodiesel B20, Aldhaidhawi et al. (2017) has been investigating the impact on engine performance and exhaust emissions on a four-stroke diesel engine. The results of a comparative study by Zehni and Saray, (2018) show that it is more efficient to use biodiesel B20 than B100 in a diesel engine. Jeon and Park investigated the effect of injection pressure on the combustion and emissions processes using Biodiesel B20. The results of the investigation show that the increase in injection pressure significantly reduces soot emissions and B20 fuel results in higher flame temperature under all injection pressure conditions. However, no studies have discussed the flame-spread behavior of B20 fuel droplets. A diesel engine is an internal combustion (IC) engine, in which fuel is sprayed into the combustion chamber in the form of liquid droplets. Preliminary studies on the evaporation rate and a single droplet of biodiesel B20 were carried out by Fitriana et al. (2018a), (2018b) but have not yet reached the combustion behavior of Biodiesel B20 droplets.

Researchers have examined the challenge of flame spread behavior by using fuels such as *n*-decane (Oyagi, et al.,

Paper No.20-00240
[DOI: 10.1299/jtst.2020jtst0024]

2009; Sano et al., 2016; Mikami et al., 2014; Mikami et al., 2017) and *n*-heptane (Farouk et al., 2014; Manzello et al., 2000) conducted in a microgravity environment. Flame spread investigation needs a microgravity environment due to limitations of the apparatus of the droplet creator. The smallest droplet that can be generated is 0.5 mm. On the other hand, the actual size of the fuel (droplets) in a spray combustion engine is very small (≤ 10 microns). Therefore, the buoyancy effect is not significant even in normal gravity. When a droplet size of 0.5 mm is burned in normal gravity, the buoyancy effect significantly influences the flame spread behavior. Sano et al. (2016) discusses the flame-spread characteristics of *n*-decane droplet arrays at different ambient pressures in microgravity. This study reported that each different ambient pressure has a different flame spread limit distance. Flame-spread behavior has been investigated through experiments and also numerical simulations. Simulations were conducted to reveal large-scale flame-spread behavior. Saputro et al., (2017) and Mikami et al., (2018) simulated the *n*-decane droplet of flame spread behavior on a large scale by using the percolation approach.

This research attempts to explore the behavior of Biodiesel B20 droplet combustion in microgravity conditions. The investigation of flame spread behavior of Biodiesel B20 droplets is very important, especially regarding the flame spread limit, flame spread time and flame spread rate

2. Experimental apparatus and procedure

The study used an experimental method to understand the combustion behavior of biodiesel (B20) droplets at room temperature and atmospheric pressure. The biodiesel used in this study has specification SNI 7182-2015 (Indonesia National Standard) as shown in Table 1. The experiment used microgravity apparatus, such as a free-fall tower (Fig. 1) and an experiment box (Fig.2). The tower generates a microgravity environment through free fall. This experiment used a 6-m high free-fall tower that has 0.93 seconds of microgravity level. The experiment box contains a droplet burning mechanism with a fixed SiC fiber (Ø= 10 μm) arrangement as the droplet to be observed. The biodiesel (B20) droplets were generated on the intersection of SiC fibers. Mikami et al., (2005) reported that there is no effect of SiC fiber on the combustion of droplets such as thermal conduction or radiative heat transfer. Retrieval of experimental data used a PENTAX Q camera with 30 frames per second (fps), which was dropped along with the experiment box.

Table 1 Biodiesel (B20) specifications based on SNI 7182-2015

No.	Test Parameter	Unit	SNI 7182-2015
1.	Density 40 ^{0}C	Kg/m^3	850-890
2.	Kinematic viscosity at 40 ^{0}C	mm^2/s (cSt)	2.3-6.0
3.	Cetane number	-	Min. 51
4.	Flash point (closed cup)	^{0}C	Min. 100
5.	Cloud point	^{0}C	Min. 18
6.	Copper strip corrosion (3 hrs, 50^{0}C)	-	Number 1
7.	Carbon residue in:		
	• Original sample	%-mass	Max. 0.05
	• or 10 residue of distillation		Max. 0.3
8.	Water and sediment	%-volume	Max. 0.05
9.	90%-distillation temperature	^{0}C	Max. 360
10.	Sulphated ash	%-mass	Max. 0.02
11.	Sulphur	mg/kg	Max. 50
12.	Phosphorous	mg/kg	Max. 4
13.	Acid value	mg-KOH/g	Max. 0.5
14.	Free Glycerol	%-mass	Max. 0.02
15.	Total Glycerol	%-mass	Max. 0.24
16.	Methyl ester content	%-mass	Min. 96.5
17.	Iodine Value	g-l_2/100g	Max. 115
18.	Oxidative Stability:		
	• Rancimat Induction Period	minute	Min. 480
	• Or Petro-Oxy Induction Period		Min 36
19.	Monoglyceride	%-mass	Max. 0.8

[DOI: 10.1299/jtst.2020jtst0024]

Fig. 1 Free fall tower at Universitas Sebelas Maret

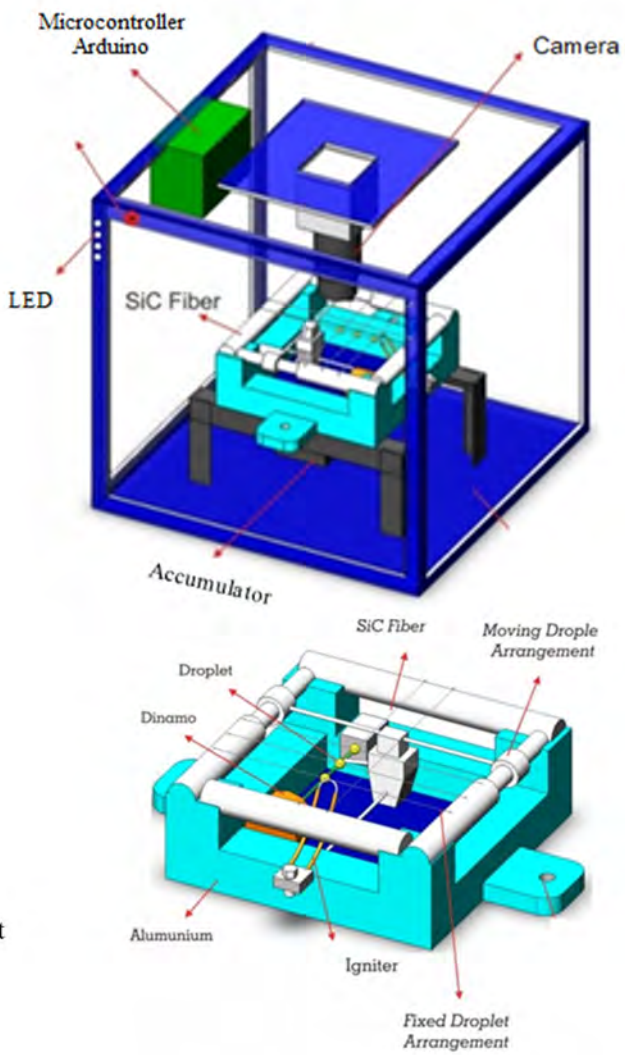

Fig. 2 Box experiment of microgravity combustion

The research was conducted in the following phases:

Phase 1: Conducting behavioral observation of a single droplet of biodiesel (B20). Observations employed various diameters of biodiesel (B20) droplets. Furthermore, the evaporation rate of Biodiesel (B20) droplets was observed.

Phase 2: Conducting behavioral observation of flame-spread from igniter droplet (Droplet A) to the Droplet B (as shown in Fig. 3). The droplet spacing A to B (S_{AB}) was normalized by the initial droplet diameter (d_{B0}) as droplet spacing (S_{AB}/d_{B0}) (Mikami et al., 2005). The droplet spacing (S_{AB}/d_{B0}) is a dimensionless. This investigation was carried out to determine the maximum distance of flame-spread from Droplets A to B without being affected by the igniter. Furthermore, Droplet B will act as a flame source to observe the flame spread limit distance of Biodiesel (B20) droplets.

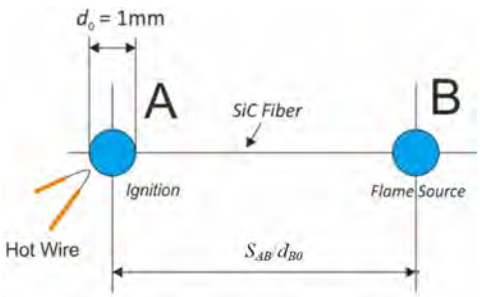

Fig. 3 The scheme of flame spread igniter droplet (Droplet A) to Droplet B

[DOI: 10.1299/jtst.2020jtst0024]

Phase 3: Conducting behavioral observation of the flame-spread limit distance from Droplet B (as flame source) to the next droplet C (as shown in Fig. 4). The droplet spacing B to C (S_{BC}) was normalized by the initial droplet diameter (d_{C0}) as droplet spacing (S_{BC}/d_{C0}). The target of this phase is to find the flame-spread mode, flame-spread limit distance ($S_{BC}/d_{C0limit}$), flame spread time and flame spread rate of Biodiesel (B20) droplets.

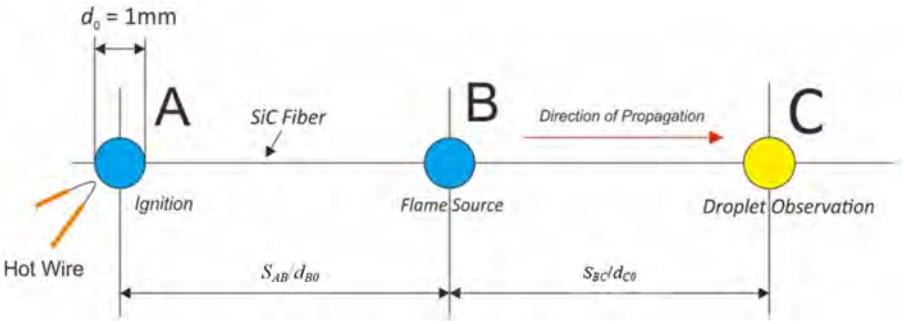

Fig. 4 The scheme of flame-spread from Droplet B (flame source) to Droplet C (observation droplet)

3. Results and discussion

3.1 Single droplet behavior of biodiesel (B20)

Observation of a single droplet of biodiesel (B20) begins with making various droplet sizes using a microsyringe, as shown in Fig. 5. The experiment was carried out with the following objectives: 1) determining how many degrees of hinges on the microsyringe must be rotated, in order to get a droplet with a diameter of 0.5, 1.0, and 1.5 mm. 2) to determine the evaporation time of biodiesel (B20) droplets at room temperature and atmospheric pressure. Figure 6 shows that to make droplet diameter Ø = 0.5, 1.0 and 1.5 mm, the handle on the microsyringe holder rotated by 1.5 ° for Ø = 0.5 mm, 12 ° for Ø = 1.0 mm, and 40 ° for Ø = 1.5 mm.

Fig. 5 Microsyringe for generate biodiesel (B20) droplet

The relation between droplet size and evaporation time was observed in detail to support the primary data of droplet behavior. Table 2 shows the measurement results of the evaporation time of Biodiesel (B20) droplets. The experimental results show that the size of the droplet diameter affects the evaporation time. The time of evaporation increases with the increase in the diameter of the droplet. Evaporation times for Biodiesel (B20) droplets of 0.5, 1.0 and 1.5 mm diameters are 1993, 6256, and 10930 minutes.

Table 2 Evaporation time of Biodiesel (B20) droplets

Droplet diameter (mm)	**Evaporation time** (minute)		
	1st	**2nd**	**3rd**
0.5	1997	1990	1993
1.0	6256	6258	6255
1.5	10930	10927	10932

[DOI: 10.1299/jtst.2020jtst0024]

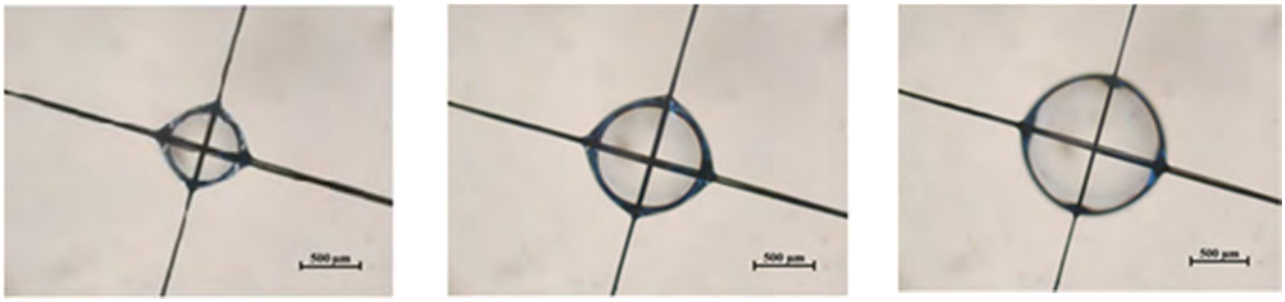

a. Biodiesel (B20) droplet Ø = 0.5 mm b. Biodiesel (B20) droplet Ø = 1.0 mm c. Biodiesel (B20) droplet Ø = 1.5 mm

Fig. 6 Experiment results of Biodiesel (B20) droplet by using microsyringe

3.2 Flame-spread behavior from Droplet A (ignition droplet) to Droplet B

The experiment was conducted to determine the flame-spread limit distance from Droplet A (ignition droplet) to Droplet B without being influenced by the igniter. This investigation was carried out to ensure that the flame spread from droplet B to droplet C (observation droplet) was not affected by hot wire. A droplet of 1-mm diameter was used in this study because it is easy to create and set up in a *SiC* fiber. Droplets A and B were arranged as shown in Fig. 3. Droplet A is an ignition droplet that was located near the igniter (hot wire). Flame-spread from Droplets A to B was observed by changing the distance and position of Droplet B. Various droplet distances from A to B (S_{AB}/d_{B0}) such as 4, 5, 6, 7 and 8 were observed as shown in Table 3 and an experiment was conducted three times at each position of Droplet B. Table 3 and Fig. 7 show that flame-spread from the ignition droplet to the next droplet until S_{AB}/d_{B0}=7 and the flame-spread has terminated for S_{AB}/d_{B0}= 8 or more than 7. This means that the flame-spread from Droplet A to the next droplet excluding hot wire ignition has the maximum flame-spread (S_{AB}/d_{B0}=7). Figures 8 and 9 show the flame spread time and flame spread rate for S_{AB}/d_{B0} =7 from droplets A to B. The figure shows that at S_{AB}/d_{B0} =7, the average flame spread time from Droplets A to B (t_{fAB}/d_{B0}^2) is 0.195 s/mm^2 and the average flame-spread rate ($V_{fAB}d_{B0}$) is 35.85 mm^2/s.

Table 3 Flame spread behavior from Droplet A (ignition droplet) to Droplet B

No	S_{AB}/d_{AB}	droplet (mm)	Experiments		
			1	2	3
1	4	1	burned	burned	burned
2	5	1	burned	burned	burned
3	6	1	burned	burned	burned
4	7	1	burned	burned	burned
5	8	1	Not burned	Not burned	Not burned

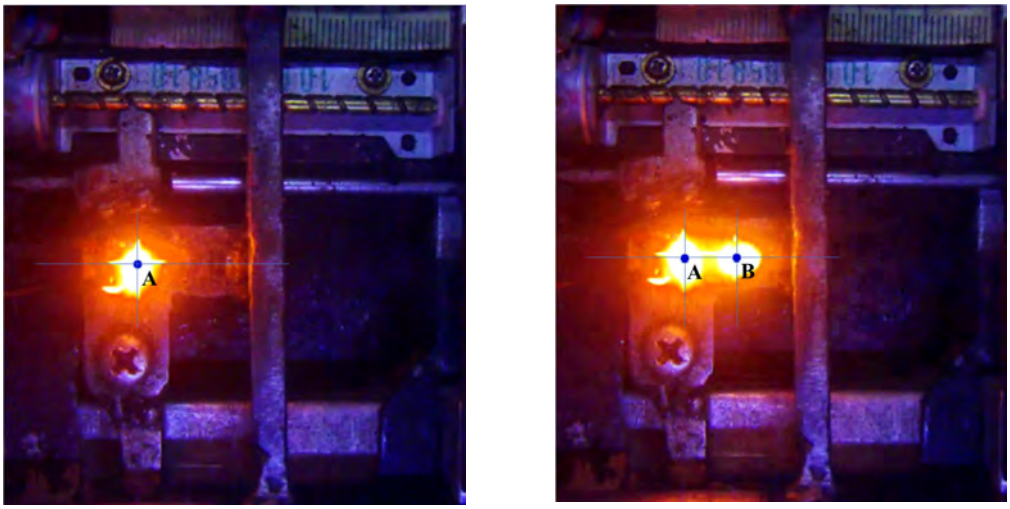

a. t_{fA} = 0.03 s b. t_{fAB} = 0.19 s

Fig. 7 Flame spread from Droplet A (ignition droplet) to Droplet B for S_{AB}/d_{B0}=7

[DOI: 10.1299/jtst.2020jtst0024]

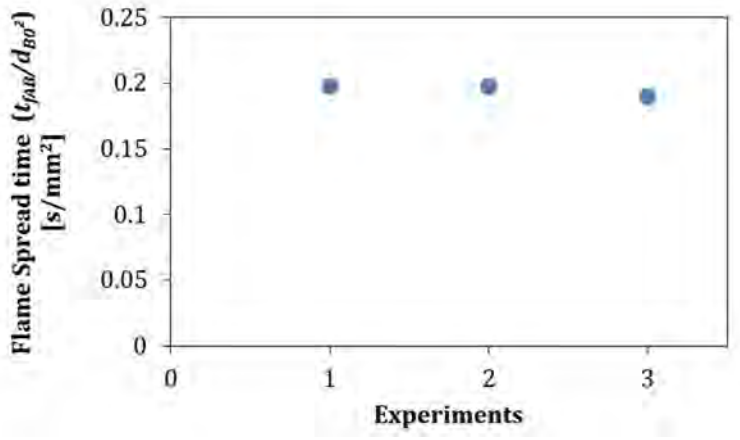

Fig. 8 Flame-spread time from Droplets A to B for S_{AB}/d_{B0}=7

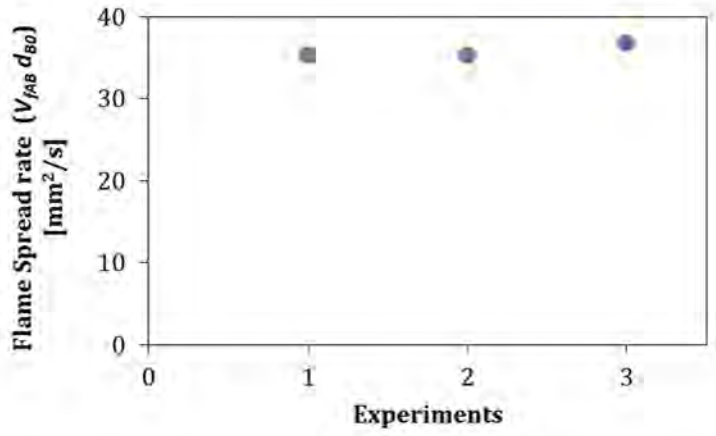

Fig. 9 Flame-spread rate from Droplets A to B for S_{AB}/d_{B0}=7

3.3 Flame spread behavior of biodiesel (B20) droplet array

The flame-spread behavior of biodiesel (B20) droplets was observed in the droplet array model at room temperature and atmospheric pressure. Droplets A, B, and C were arranged as shown in Fig. 4. The location of the ignition Droplet A was fixed, while Droplet B was placed 7 mm from Droplet A. Flame-spread from Droplets B to C was observed by changing the distance and position of Droplet C (observation droplet). The flame-spread behavior of biodiesel (B20) from droplet B to C discussed in detail, such as: 1) flame-spread mode based on Mikami et al. 2006, 2) flame-spread limit distance $S_{BC}/d_{C0\ limit}$ or we identify as $(S/d_0)_{limit}$ of biodiesel (B20) droplets, and 3) flame-spread time and flame-spread rate.

3.3.1 Flame-spread mode of biodiesel (B20) droplet

We observed the flame spread mode of biodiesel (B20) droplets. Figure 10.a shows the sequential images and leading edge position of flame spread from droplets B to C for S_{BC}/d_{C0} = 4. The results of flame-spread from droplets B to C for S_{BC}/d_{C0} = 4 is categorized “Mode 1 flame-spread”. The characteristic of mode 1 is the next unburned droplet (droplet C) is swallowed by the expanding diffusion flame of droplet B and start to vaporize actively, as shown in Fig. 10.b. Finally the flame spread from droplet B pushed the leading edge forwards to droplet C (Fig. 10.b). In this mode, the next unburned droplet got the enough heating to vaporize actively from the expanding diffusion flame and the droplet heating mainly controls the flame-spread. When the S_{BC}/d_{C0} is relatively small the Mode 1 flame-spread and group combustion occurs. Group combustion is defined as the burning mode which occurrence merged flame from burning droplets in the combustion chamber. The occurrence of group combustion in fuel spray combustion is necessary to attain a stable flame in combustors.

[DOI: 10.1299/jtst.2020jtst0024]

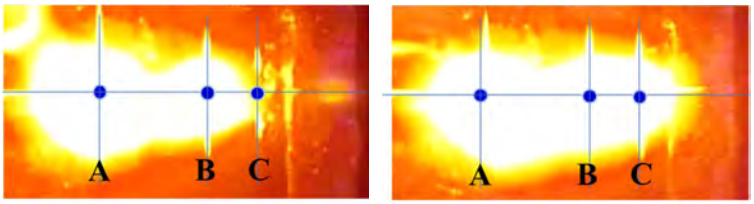

t=0.27 s/mm t=0.32 s/mm

(a) Experiment results S_{BC}/d_{C0} = 4

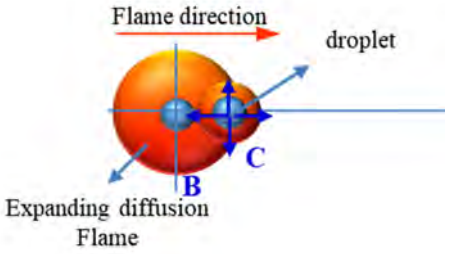

(b) Illustration of mode 1 flame spread

Fig. 10 The flame spread mode of droplets B to C for S_{BC}/d_{C0} = 4 and illustration of "Mode 1 flame spread"

Figure 11.a shows the characteristic of flame-spread mode for S_{BC}/d_{C0} = 5. The results informed that flame-spread from droplets B to C for S_{BC}/d_{C0} = 5 is categorized "Mode 2 flame-spread". This is due to the leading edge of the diffusion flame of droplet B reaches the flammable mixture layer formed around the next droplet (droplet C) and the premixed flame propagates in the mixture layer to form the diffusion flame around the next droplet as illustrated in Fig.11.b. The heat is transferred from the leading edge of the diffusion flame of droplet B to the next unburned droplet C, but the droplet heating mainly controls the flame-spread. The flame-spread behavior form droplet B to C for S_{BC}/d_{C0} = 5 shown the occurrence of group combustion.

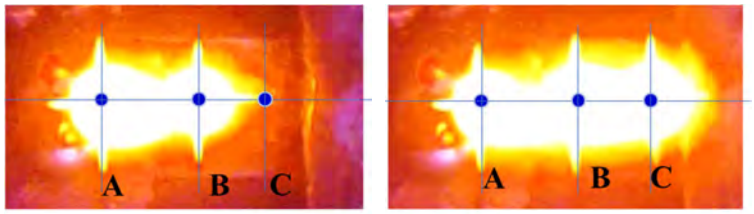

t=0.27 s/mm t=0.36 s/mm

(a) Experiment results S_{BC}/d_{C0} = 5

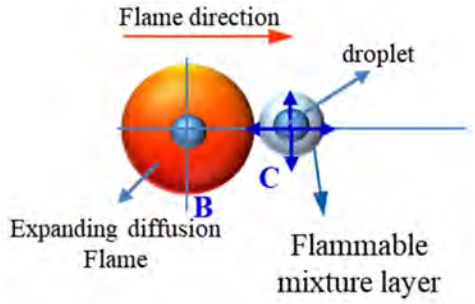

(b) Illustration of mode 2 flame spread

Fig. 11 The flame spread mode of droplets B to C for S_{BC}/d_{C0} = 5 and illustration of "Mode 2 flame spread"

The flame-spread behavior of droplets B to C for S_{BC}/d_{C0} = 7 shown in Fig. 12.a. The Figure revealed that the "Mode 3 flame-spread" i.e. the droplet C auto ignites through heating by the diffusion flame from droplet B, whose leading-edge does not reach the flammable-mixture layer around the next droplet C. In this mode the heat is transferred from the leading edge of the diffusion flame (droplet B) to the next unburned droplet C through the thermal conduction

[DOI: 10.1299/jtst.2020jtst0024]

as illustrated in Fig. 12.b. Therefore, the thermal conduction mainly controlled the flame-spread of droplet B to C. The flame-spread behavior form droplet B to C for S_{BC}/d_{C0} = 5 shown the transition from individual combustion to group combustion.

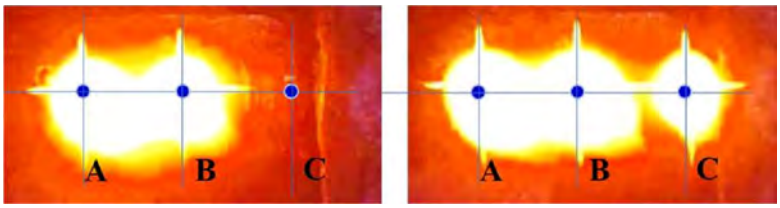

t=0.30 s/mm t=0.41 s/mm

(a) Experiment results S_{BC}/d_{C0} = 7

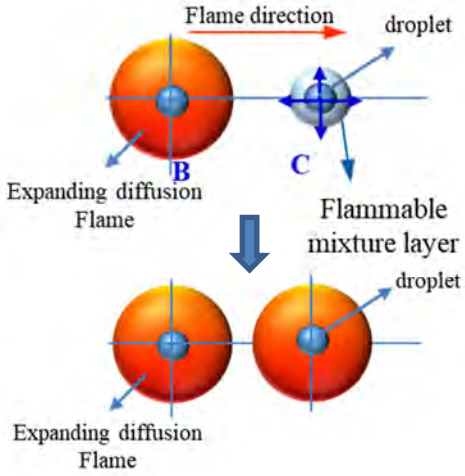

(b) Illustration of mode 3 flame spread

Fig. 12 The flame spread mode of droplets B to C for S_{BC}/d_{C0} = 7 and illustration of "Mode 3 flame spread"

The vaporization mode occurs when the thermal conduction from the flame of droplet B cannot diffusion and spread to the next droplet C, as shown in Fig. 13.a. In this experiment, the vaporization mode occurs when the S_{BC}/d_{C0}= 8 which is the flame-spread has terminated and flame-spread does not occur as illustrated in Fig. 13.b.

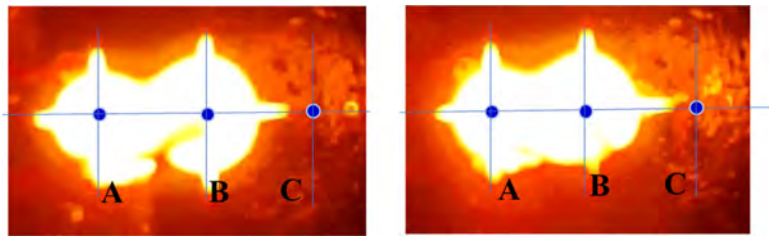

t=0.32 s/mm t=0.42 s/mm

(a) Experiment results S_{BC}/d_{BC} = 8

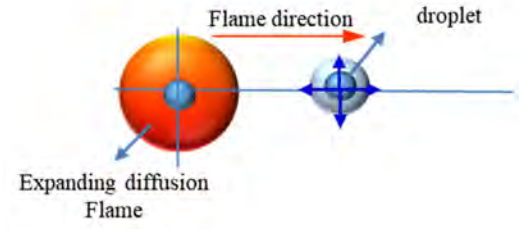

(b) Illustration of vaporization mode

Fig. 13 The flame spread mode of droplets B to C for S_{BC}/d_{C0} = 8 and illustration of "vaporization mode"

[DOI: 10.1299/jtst.2020jtst0024]

3.3.2 Flame-spread limit distance of biodiesel (B20) droplet

Based on the relationship between the droplet spacing (S_{BC}/d_{C0}) and flame-spread behavior and mode, it can be seen that the maximum distance of flame-spread from the droplet B to C. The flame-spread characteristic of biodiesel (B20) droplets are the flame spread to the next unburned droplet for the $S_{BC}/d_{C0} \leq 7$ and the flame-spread has terminated for the $S_{BC}/d_{C0} > 7$. Therefore, the $S_{BC}/d_{C0} = 7$ become the boundary between Mode 3 flame-spread and vaporization mode. The boundary was identified as the flame-spread limit distance ($S_{BC}/d_{C0\ limit}$). The flame-spread at boundary region $S_{BC}/d_{C0} = 7$ was controlled by the thermal conduction of burned droplet B. The flame-spread limit distance $S_{BC}/d_{C0\ limit}$ of biodiesel (B20) droplets occurred when the distance of droplet B to C (S_{BC}) = 7 mm and the droplets diameter C (d_{C0}) = 1mm or $S_{BC}/d_{C0\ limit} = 7$. The results of this experiment show that the parameter of droplet spacing (S_{BC}/d_{C0}) affects to the flame-spread mode of biodiesel (B20) droplets. When the S_{BC}/d_{C0} is relatively small the "Mode 1 or 2" flame-spread occurs and when the S_{BC}/d_{C0} is increased until less than the flame-spread limit distance ($S_{BC}/d_{C0\ limit}$), the mode 3 flame-spread occurs. When the S_{BC}/d_{C0} is greater than the flame-spread limit distance ($S_{BC}/d_{C0\ limit}$), the vaporization mode occurs.

3.3.3 Flame-spread flame-spread time and rate of biodiesel (B20) droplet

Last, we observed the flame-spread time (t_{fBC}) and flame-spread rate (V_{fBC}) of biodiesel (B20) droplets. The flame-spread time t_{fBC} and flame-spread rate are normalized by the initial droplet diameter of droplet C as flame-spread time (t_{fBC}/d_{C0}^2) and flame-spread rate ($V_{fBC}d_{C0}$) (Mikami et al., 2018). The t_{fBC}/d_{C0}^2 and $V_{fBC}d_{C0}$ was measured at various droplets spacing i.e. 4, 5, 6, and 7 mm. Figure 14 shows the results of the flame-spread time from Droplets B to C. Flame-spread time (t_{fBC}/d_{C0}^2) was defined as time that was measured starting the ignition of droplet B and flame propagate to the droplet C until ignition occurs. When the S_{BC}/d_{C0} relatively small, the flame can spread quickly from Droplets B to C and a group flame occurred in this condition as shown in Fig. 10 and the flame-spread time increasing when the droplet spacing was increased until less than the flame-spread limit distance ($S_{BC}/d_{C0\ limit}$)

Figure 15 shows the results of normalized flame-spread rate ($V_{fBC}d_{C0}$) as function of droplets spacing (S_{BC}/d_{C0}). The flame-spread rate ($V_{fBC}d_{C0}$) significantly decreasing when the droplets spacing (S_{BC}/d_{C0}) increasing. The case of $S_{BC}/d_{C0} = 4$ revealed that the highest value of flame-spread rate ($V_{fBC}d_{C0}$). This is due to the next unburned droplet C is swallowed by the expanding diffusion flame of droplet B and the group combustion occurred. However, the case of $S_{BC}/d_{C0} = 7$ shown that the lower value of $V_{fBC}d_{C0}$ than the other droplets spacing (S_{BC}/d_{C0}). When the droplets spacing (S_{BC}/d_{C0}) was increases until less than the flame-spread limit distance ($S_{BC}/d_{C0\ limit}$), the flame-spread time for the heat transfer from the burned droplets to the next unburned droplets also increases, as shown in Fig. 14. Based on the experiment results of flame-spread behavior and mode, we conclude that the flame-spread of biodiesel (B20) droplets is controlled by the thermal conduction. Therefore, the flame-spread rate has a maximum value for specific droplets spacing.

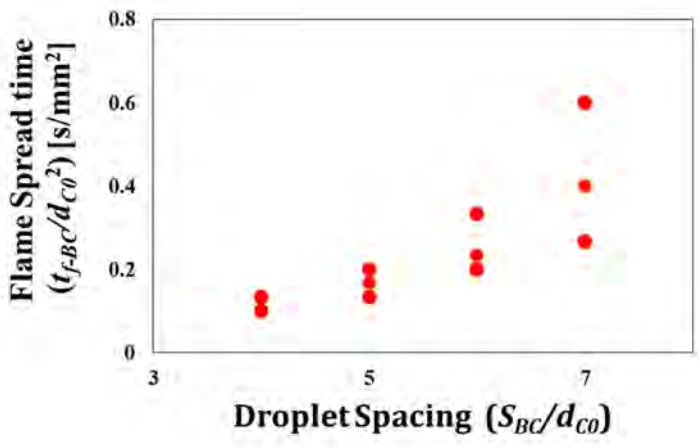

Fig. 14 Dependence of flame-spread time from Droplets B to C (t_{fBC}/d_{C0}^2) at room temperature on droplet spacing (S_{BC}/d_{C0})

[DOI: 10.1299/jtst.2020jtst0024]

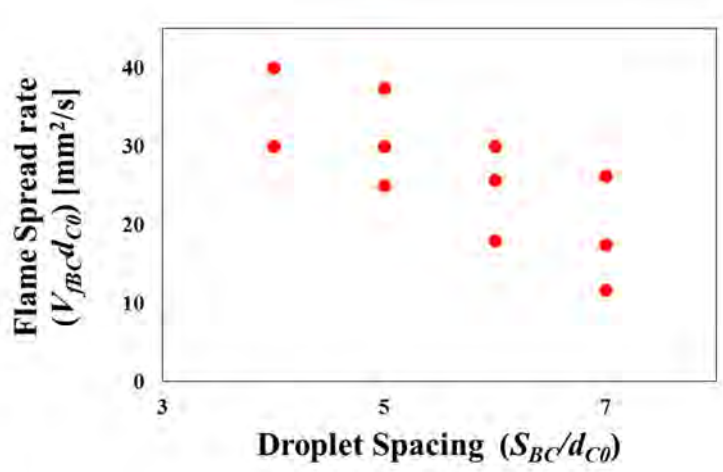

Fig. 15 Dependence of flame-spread rate from Droplets B to C (t_{fBC}/d_{C0}^2) at room temperature on droplet spacing (S_{BC}/d_{C0})

4. Conclusions

In this research, the behavior of the flame-spread of Biodiesel (B20) droplets was observed. This study focused on the behavior of the single droplet and the flame spread of the biodiesel (B20) droplet array model at room temperature and atmospheric pressure. The conclusions of this study are as follows:

a. Biodiesel (B20) droplets have a fairly long evaporation time for each diameter at room temperature and atmospheric pressure. The evaporation times for Biodiesel (B20) droplets of 0.5, 1.0 and 1.5 diameters are 1993, 6256 and 10930 minutes. The evaporation time increases with the increase in the diameter of the droplet.

b. The placement of Droplet B or droplets that will act as a flame source for the observation flame-spread limit distance of biodiesel (B20) can be placed on the $S_{AB}/d_{B0} = 7$ from the ignition droplets (Droplet A). This is due to the flame-spread from Droplet A to the next droplet excluding the hot wire ignition.

c. The parameter of droplet spacing (S_{BC}/d_{C0}) affects to the flame-spread mode of biodiesel (B20) droplets. When the (S_{BC}/d_{C0}) is relatively small the "Mode 1 or 2 flame-spread" occurs and when the (S/d_0) is increased until less than the ($S_{BC}/d_{C0\ limit}$) the "Mode 3 flame spread occurs". When the (S_{BC}/d_{C0}) is greater than the ($S_{BC}/d_{C0\ limit}$), the vaporization mode occurs.

d. The flame-spread limit distance of the biodiesel (B20) droplet in the droplet array model at room temperature and atmospheric pressure ($S_{BC}/d_{C0\ limit}$) = 7

Acknowledgements

This research was partly subsidized by a grant of international collaboration research from PNPB Universitas Sebelas Maret 2019. The researchers gratefully acknowledge financial support from the LPPM Universitas Sebelas Maret, Surakarta, Indonesia.

References

Aldhaidhawi, M., Chiriac, R., Badescu, V., Descombes, G. and Podevin. P., Investigation on the mixture formation, combustion characteristics and performance of a Diesel engine fueled with Diesel, Biodiesel B20 and hydrogen addition, International Journal of Hydrogen Energy, Vol. 42, No.26 (2017), pp.16793-16807, DOI: 10.1016/j.ijhydene.2017.01.222.

Ambat, I., Srivastava, V. and Sillanpää, M., Recent advancement in biodiesel production methodologies using various feedstock: A review, Renewable and Sustainable Energy Reviews, Vol. 90, (2018), pp.356–369, DOI:

10.1016/j.rser.2018.03.069.

Farouk, T.I. and Dryer, F. L., Isolated n-heptane droplet combustion in microgravity: “Cool Flames” - Two-stage combustion, Combustion and Flame, Vol.161, No.2 (2014), pp.565–581, DOI: 10.1016/j.combustflame.2013.09.011.

Fitriana, L., Gumelar, W. B., Saputro, H., Firdani, T., Muslim, R. and Setyaningrum, H., Study experimental of flame-spread rate and spread limit distance of bio-solar droplets in microgravity combustion, MATEC Web of Conferences, Vol. 197, (2018a), DOI: 10.1051/matecconf/201819708006.

Fitriana, L., Nugroho R A A, Saputro, H., Firdani, T., Muslim, R., Gumelar W. B., Setyaningrum, H., Ismunandar, H. A., Zainudin, R. A., Rahmadi, W. and Sutrisno, V. L. P., The basic investigation of evaporation rate and burning temperature of various type of liquid fuels droplet, IOP Conference Series: Materials Science and Engineering, Vol. 434 (2018b), DOI: 10.1088/1757-899X/434/1/012182.

Jeon, J. and Park, S., Effect of injection pressure on soot formation/oxidation characteristics using a two-color photometric method in a compression-ignition engine fueled with biodiesel blend (B20), Applied Thermal Engineering, Vol.131, (2018), pp.284–294, DOI: 10.1016/j.applthermaleng.2017.12.005.

Knothe, G. and Razon, L. F., Biodiesel fuels. Progress in Energy and Combustion Science, Vol. 58, (2017), pp.36–59, DOI: 10.1016/j.pecs.2016.08.001.

Kumar, S. R, Sureshkumar, K. and Velraj, R., Combustion, performance and emission characteristics of an unmodified diesel engine fueled with Manilkara Zapota Methyl Ester and its diesel blends, Applied Thermal Engineering, Vol.139 (2018), pp.196–202, DOI: 10.1016/j.applthermaleng.2018.04.107.

Nabi, M. N. and Rasul, M. G., Influence of second generation biodiesel on engine performance, emissions, energy and exergy parameters, Energy Conversion and Management, Vol. 169, (2018), pp.326–233, DOI: 10.1016/j.enconman.2018.05.066.

National Renewable Energy Laboratory (NREL), Biodiesel Handling and Use Guide, Fourth Edition, NREL/TP-540-43672, (2009).

Manzello, S.L., Choi, M.Y., Kazakov, A., Dryer, F. L., Dobashi, R. and Hirano, T., The burning of large n-heptane droplets in microgravity, Proceedings of the Combustion Institute, Vol.28, No.1 (2000), pp.1079–1086, DOI: 10.1016/S0082-0784(00)80317-3

Mikami, M., Oyagi, H., Kojima, N., Kikuchi, M., Wakashima, Y. and Yoda, S., Microgravity experiment on flame spread along fuel-droplet array using a new droplet-generation technique, Combustion and Flame, Vol.141, No.3 (2005), pp. 241–252, DOI: 10.1016/j.combustflame.2005.01.007

Mikami, M., Oyagi, H., Kojima, N., Wakashima, Y., Kikuchi, M. and Yoda, S., Microgravity experiment on flame spread along fuel-droplet arrays at high temperature, Combustion and Flame, Vol. 146, No.3 (2006), pp. 391-406, DOI: 10.1016/j.combustflame.2006.06.004.

Mikami, M., Sano, N., Saputro, H., Watari, H. and Seo, T., Microgravity Experiment of Flame Spread over Droplets at Low Pressure, International Journal of Microgravity Science and Application, Vol.31, No.4 (2014), pp. 172–178, DOI: 10.15011/jasma.31.4.172.

Mikami, M., Saputro, H., Seo, T. dan Oyagi, H., Flame Spread and Group-Combustion Excitation in Randomly Distributed Droplet Clouds with Low-Volatility Fuel near the Excitation Limit: a Percolation Approach Based on Flame-Spread Characteristics in Microgravity, Microgravity Science and Technology, Vol.30 (2018), pp. 419-433.

Mikami, M., Watari, H., Hirose, T., Seo, T., Saputro, H., Moriue, O. and Kikuchi, M., Flame spread of droplet-cloud elements with two-droplet interaction in microgravity, Journal of Thermal Science and Technology, Vol. 12, No.2 (2017), pp. 1 -10, DOI: 10.1299/jtst.2017jtst0028.

Oyagi, H., Shigeno, H., Mikami, M. and Kojima, N., Flame-spread probability and local interactive effects in randomly arranged fuel-droplet arrays in microgravity, Combust Flame,Vol.156, No.4 (2009), pp.763–770, DOI: 10.1016/j.combustflame.2008.12.013

Saluja, R. K., Kumar, V. and Sham, R., Stability of biodiesel – A review, Renewable and Sustainable Energy Reviews,, Vol. 62 (2016), pp.866 – 881, DOI: 10.1016/j.rser.2016.05.001

Sano, N., Motomatsu, N., Saputro, H., Seo, T. and Mikami, M., Flame-Spread Characteristics of n-Decane Droplet Arrays at Different Ambient Pressures in Microgravity, International Journal of Microgravity Science and Application, Vol.33, No.1 (2016), pp. 1-5, DOI: 10.15011/ijmsa.33.330108.

Saputro, H., Fitriana, L., Mikami, M. and Seo, T., Group Combustion Excitation in Randomly Distributed Droplet

Clouds Based on Flame-spread Characteristics with Two-droplet Interaction in Microgravity, SAE Technical Paper, 32-007, (2017).

Suresh, M., Jawahar, C. P. and Richard, A., A review on biodiesel production, combustion, performance, and emission characteristics of non-edible oils in variable compression ratio diesel engine using biodiesel and its blends, Renewable and Sustainable Energy Reviews, Vol.92, (2018), pp. 38–49, DOI: 10.1016/j.rser.2018.04.048.

Zehni, A. and Saray, R. K., Comparison of late PCCI combustion, performance and emissions of diesel engine for B20 and B100 fuels by Kiva-Chemkin coupling, Renewable Energy, Vol.122, (2018), pp.118–130, DOI: 10.1016/j.renene.2018.01.046.

[DOI: 10.1299/jtst.2020jtst0024]